marily by shape, then both light curves would show simultaneous maxima when the broad side of Hektor faces the observer. However, if the light curve is due to albedo patches, then the maximum in reflected sunlight would correspond to the bright or cooler side, which would produce a minimum in the thermal infrared curve. Therefore the two light curves would be correlated in phase if due to elongated shape, but anticorrelated if due primarily to albedo patches.

The amplitudes would also be different in the two cases. If the light curve is due to elongated shape, the amplitude would measure essentially the cross-sectional area exposed (modulated by any minor albedo patchiness). But if an albedo effect dominates in producing the reflected light amplitude, then the amplitude of the infrared light curve would depend on the temperature difference between the markings, and this in turn would depend on the absolute range of albedos. In the case of Hektor this must be very small, since its average albedo is about 2 to 3 percent (*2, 3*). If we assume the albedos of the two hemispheres, with a ratio of 3.1, to be approximately 0.012 and 0.038, then the light absorbed by the different regions of Hektor varies between 0.96 and 0.99, producing a thermal light curve amplitude of only about 1.02:1. (Alternatively, had Hektor been highly reflective—for example, with albedo of 0.86 on one side and 0.28 on the other—the thermal light curve amplitude could exceed 5:1.)

On 4 and 5 April 1979 we obtained new light curves with the 224-cm telescope at Mauna Kea Observatory, when Hektor's brightness was varying by about a factor of 2. The reflected sunlight was represented by photometry at 1.2 μm, and the thermal infrared radiation was represented by photometry at an effective wavelength of 20 μm. Using the known rotation period (*1*), we combined the photometric data from the two nights into a single rotational light curve, shown in Fig. 1.

The primary standard for the 1.2-μm observations was θ Leonis, for which $m_J = 3.34$; the standard for the 20-μm observations was R Hydrae, for which $m_Q = -4.76$. The data in Fig. 1 were obtained in the beam-switching mode with modulation of the asteroid signal against that from the background sky by the standard method of infrared photometry. Each J point is the mean of 240 seconds of integration, and each Q point is the mean of 400 seconds.

Figure 1 establishes that the maxima and minima of the two light curves are correlated, not anticorrelated, and have the same amplitude within the limits of measurement. This, in turn, shows that 624 Hektor must have an elongated shape, which accounts for most of the light variation.

In proposing our model for Hektor (*3*), we pointed out that a compound asteroid consisting of two uniform spheres could not have a light curve amplitude greater than 2:1. Indeed, the original model by Dunlap and Gehrels (*1*) called for a more elongated, cigar-shaped object to explain the observed light curve, which can reach an amplitude of 3.1:1 when Hektor is viewed in its equatorial plane. Therefore we proposed that the crushed material in the contact zone between the two components may be brighter material, analogous to rays around fresh lunar craters. Because of the weak influence of albedo on photometry, this "ray" material would be difficult to detect by photometry alone, but might be spectrophotometrically apparent. At any rate, the material exposed in the side view may be different from that seen in the end views, providing a test of the model. Further, if Hektor formed from two distinct asteroids, the materials seen in the two end views (views of the two original objects) may be different from each other. Since our new results confirm the peculiarity of Hektor's shape and are consistent with our hypothesis (*3*), it is important to follow up with further spectrophotometric observations that might confirm such predicted composition differences.

Interestingly, Jupiter's inner satellite Amalthea was revealed by Voyagers 1 and 2 to be a distinctly Hektor-like object measuring about 155 by 170 by 270 km, or about 83 to 91 percent of the estimated length of Hektor (*6*). In view of its proximity to at least one other small satellite and a ring system of debris, as well as a meteoroid flux enhanced by Jupiter's gravity, Amalthea's collisional history and possible origin as a fragment or a compound object are difficult to assess.

The question of Hektor's origin thus remains puzzling and unresolved, but Hektor may be a fossilized example of the primitive collisional accretion process. In any case, we have established that Hektor is the most elongated object of its size and that it is a worthy candidate for future study or possible spacecraft exploration.

WILLIAM K. HARTMANN
Planetary Science Institute, Tucson, Arizona 85719
DALE P. CRUIKSHANK
Institute for Astronomy, University of Hawaii, Honolulu 96822

References and Notes

1. J. L. Dunlap and T. Gehrels, *Astron. J.* **74**, 797 (1969).
2. D. P. Cruikshank, *Icarus* **30**, 224 (1977).
3. W. K. Hartmann and D. P. Cruikshank, *ibid.* **36**, 353 (1978).
4. J. Degewij, *Proc. 8th Lunar Sci. Conf.* **1**, 145 (1977); thesis, Leiden University (1978).
5. W. K. Hartmann, in *Asteroids*, T. Gehrels, Ed. (Univ. of Arizona Press, Tucson, 1979).
6. B. A. Smith *et al.*, *Science* **206**, 927 (1979).
7. This work was supported by NASA's Planetary Astronomy program through NASA contract NASW-3134 (Planetary Science Institute) and NASA grant NGL-12-001-054 (University of Hawaii). This is Planetary Science Institute Contribution 135.

16 November 1979

Electron Spin Resonance Dating of Animal and Human Bones

Abstract. *Ages of fossil bones were determined by electron spin resonance spectroscopy. The electron spin resonance signal is associated with lattice defects or trapped centers produced by natural radiation in the bones and gives a measure of the total dose of natural radiation, or the archeological dose. Archeological doses were determined for samples of known age from a variety of sites and used to estimate apparent average annual rates of natural radiation at the sites. The method has the advantage that the sample need not be ground or heated, and it should be useful for dating biological materials.*

Natural radiation from uranium, thorium, potassium and their radioactive daughters produces lattice defects or populates existing and radiation-induced electron traps with electrons and holes (*1, 2*). One can determine the total dose of natural radiation, or the archeological dose, from the concentration of defects or traps. Thermoluminescence has been used to obtain the archeological dose, and thermoluminescence dating of potteries and ceramics in archeology has been attempted by several groups (*1, 2*). Jasinska and Niewiadomski (*3*) tried thermoluminescence dating of fossil bones and some biological material; samples exhibited triboluminescence due to defect formation during grinding and chemiluminescence due to oxidation of the residual organic materials during heating.

Electron spin resonance (ESR) of defects or trapped centers produced by natural radiation has been successfully used to estimate the age of the deposits such as stalactites in calcite caves and of min-

0036-8075/80/0229-0977$00.50/0

erals such as apatites (*4*, *5*). It utilizes microwave absorption by paramagnetic centers in solids in a magnetic field. For dating biological material, ESR has the advantages that it is not necessary to grind the sample into a fine powder and one can make the measurements repeatedly at room temperature; thus interference from triboluminescence and chemiluminescence is not a problem.

In this report, we demonstrate the validity of ESR dating of animal and human bones. We used ESR to determine the archeological doses of bones from different excavation sites whose ages are known archeologically or historically and are in the range 10^2 to 10^6 years. By comparing these doses with the known ages of the bones, we obtained an apparent annual rate of natural radiation of about 1 rad per year for bones at an open site and 0.1 to 0.2 rad per year for bones in a calcite cave. Thus, the age of human and animal bones can be estimated from the archeological dose determined by ESR without accurately measuring the radioactive elements and accumulation processes in the bones.

Figure 1 shows a typical ESR derivative line of a fossil bone. A signal with a value for the g factor of 2.002 is associated with the radicals created by the natural radiation. The six lines associated with the hyperfine line of Mn^{2+} are indicated in Fig. 1. Before the ESR measurements, the bone marrow and especially the brown muddy portion of the surface were cut away; the contamination gives a broad ESR signal, presumably associated with paramagnetic iron and other impurities. The signal intensity at $g = 2.002$ was measured relative to the signal intensity of Mn^{2+}. In some cases where no Mn^{2+} signal was detected, a standard sample of calcite with Mn^{2+} was measured together with the bone sample. The g value of the radical signal agrees with that of apatite, which was first detected by Zeller and co-workers (*5*, *6*) in a thermal annealing study of a natural apatite crystal. The ESR intensity of the radical signal is enhanced by artificial γ irradiation.

It is interesting to note that the bones of atomic bomb victims at Hiroshima show the presence of similar ESR signals due to defects in the apatite structures (*7*). Radicals of the O^- type are created by radiation in synthetic hydroxyapatite crystals. X-ray diffraction of the bones excavated by anthropologists shows the pattern of the apatite structure. Thus the radicals, presumably of the O^- type, produced by natural radiation in hydroxyapatite would be responsible for the ESR signal of bones.

Figure 2 shows the enhancement of the ESR signal of animal bones induced by ^{60}Co γ irradiation. The data are for deer and wild pig bones excavated at the Kidosaku shell mound in Japan. A linear signal increase induced by γ irradiation was observed up to about 10^6 rads. Least-squares fits of the data gave values for the archeological dose of 4.2×10^3 rads for two different deer bones and 4.8×10^3 rads for the pig bone. The ages of bones excavated at the same site were determined by ^{14}C dating to be 3500 ± 50 years; these bones were embedded in a fertile soil.

To estimate the annual radiation dose to the bones, their total content of radioactive elements must be accurately measured. It is known that radioactive elements, especially ^{238}U, build up in fossil bones. Uranium uptake and fluorination of hydroxyapatite complicate the estimation of the average content of radioactive elements. The efficiency of radical production by artificial γ-rays is different from that by α, β, and γ radiation from the radioactive elements in the bones and in the environment. In this report, we present only the ^{60}Co γ-ray equivalent archeological dose of animal and human bones whose age is known historically or has been determined by other methods, including ^{14}C dating.

Figure 3 shows a logarithmic plot of human and animal bone archeological doses determined by ESR as a function of the age determined by other measurements. Annual radiation doses of 0.1, 0.2, and 1.0 rad per year are indicated by dashed lines of slope 1.0. Some bones are from calcite caves, where the content of radioactive elements in the environment is considered low (*4*). The youngest age measured was for a human bone buried in 1333; the archeological dose obtained by ESR is about 700 rads. The oldest bones measured were supplied by the Greek Anthropology Association and are believed to be about 700,000 years old. Other human and animal bones were supplied by the Anthropology Department of Tokyo University and by the Natural History Museum at Stuttgart. These are from Japanese shell mounds and caves or Serian caves excavated by Tokyo University and from Steinheim excavation sites in Germany. Except for the bones older than 50,000 years, all the

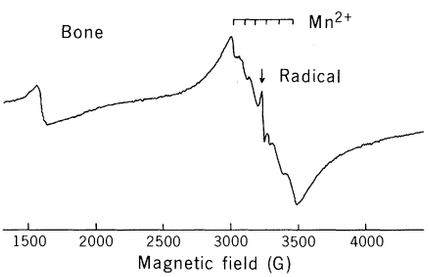

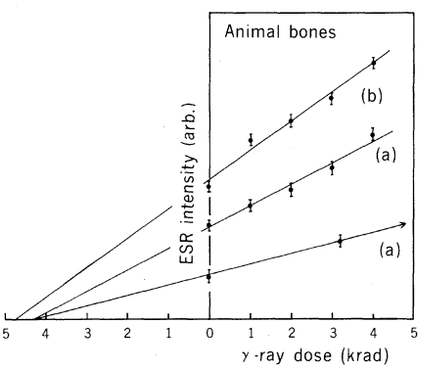

Fig. 1 (left). Typical ESR spectrum of an old animal bone. The arrow indicates the radical signal at $g = 2.002$. Fig. 2 (right). Growth of the ESR signal of (a) deer bones and (b) wild pig bones at Kidosaku shell mound in Japan with artificial γ irradiation. The archeological dose is obtained by extrapolating the growth of the signal.

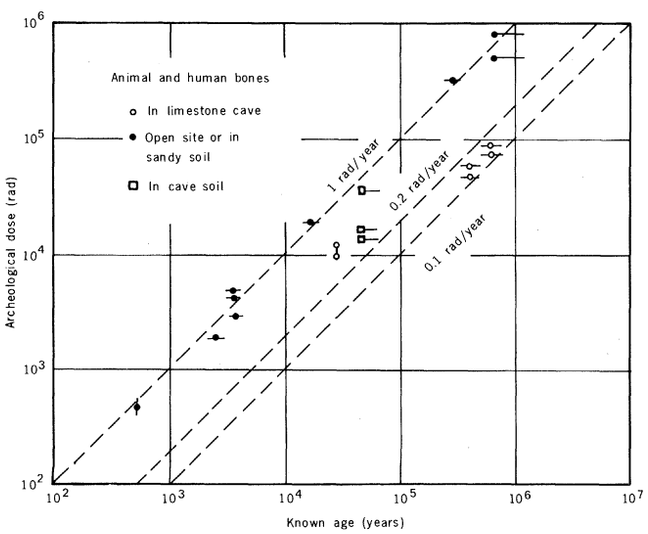

Fig. 3. Archeological dose of animal and human bones as a function of the age, known historically or determined by other methods. Apparent annual doses of 0.1, 0.2, and 1 rad per year are indicated by dashed lines.

ages indicated were determined by ^{14}C dating or historically. The error bars indicate the uncertainty in age, based on other methods of dating such as fission track dating and on circumstantial evidence. Bones believed to be older on the basis of their stratigraphic location gave equal or larger archeological doses in many cases.

The annual dose was about 0.1 to 0.2 rad per year for cave formations such as stalactites and stalagmites (*4*); this dose rate also seems appropriate for bones excavated from calcite caves. A dose rate of about 1 rad per year fits the data for bones embedded in sandy soil or open sites. However, it is known that uranium and other elements accumulate in these bones, and in some cases uranium concentrations of 10 to 100 parts per million have been measured in old bones. The annual dose rate should be higher than 1 rad per year on the basis of the energies of α, β, and γ radiation from the elements in the ^{238}U and ^{232}Th disintegration series, assuming that the parents and daughters are in equilibrium. It should be noted that fluorination of apatite in bone proceeds continuously, and therefore the production rate of radicals, presumably of the O^- type in hydroxyapatite, diminishes considerably with time. Thus our finding that bones from exposed sites can be dated from the archeological dose by using an apparent annual dose of 1 rad per year might indicate an equilibrium between an enhancement due to radiation-induced defect or trap formation and a reduction due to impurity accumulation or fluorination of hydroxyapatite.

We conclude that ESR dating of bones and similar biological materials should be useful in archeology and anthropology, especially when thermoluminescence dating is difficult. Ages ranging from hundreds to millions of years can be deduced without difficulty. Carbon-14 dating is limited to about 50,000 years. However, application to geological materials (*6*) might be difficult, as the ESR signal, which is increased by artificial radiation, is saturated at high-dose regions (about 10^6 to 10^7 rads). Thermal stability data for radiation-induced defects and traps at room temperature indicate that they should be stable for millions of years, at least in bones. Only a few geological materials with low concentrations of radioactive elements and with high stability of defects and traps may be dated by ESR, as demonstrated for apatite crystals (*6*).

MOTOJI IKEYA
TOSHIKATSU MIKI
Technical College, Yamaguchi University, Ube 755, Japan

References and Notes

1. M. U. Aitken, *Physics in Archaeology* (Clarendon, Oxford, ed. 2, 1974).
2. P. W. Levy, in *Proceedings of the International Seminar on the Application of Science to the Dating of Works of Art*, W. J. Young, Ed. (Museum of Fine Arts, Boston, 1978), p. 9.
3. M. Jasinska and T. Niewiadomski, *Nature (London)* **227**, 1159 (1971).
4. M. Ikeya, *ibid.* **255**, 48 (1975); *Archaeometry* **20**, 149 (1978).
5. E. J. Zeller, P. W. Levy, P. L. Mattern, in *Proceedings of the Symposium on Radioactive Dating and Low-Level Counting* (International Atomic Energy Agency, Vienna, 1967), p. 531.
6. E. J. Zeller, in *Thermoluminescence of Geological Materials*, D. J. McDougall, Ed. (Academic Press, London, 1968), p. 271.
7. S. Mascarenhas, A. Hasegawa, K. Takeshita, *Bull. Am. Phys. Soc.* **18**, 579 (1973).
8. We thank N. Watanabe, S. Matsura, S. Akazawa, A. Poulianos, R. D. Adams, and H. Pick for supplying the samples. This work was supported by the Yamada Science Foundation and was performed partly at the Reactor Institute of Kyoto University and at the Physics Institute of the University of Stuttgart, where M.I. was a research fellow of the Alexander von Humbolt Foundation.

28 August 1979; revised 8 November 1979

Isotopic Disequilibrium of Uranium: Alpha-Recoil Damage and Preferential Solution Effects

Abstract. *Preferential loss of uranium-234 relative to uranium-238 from rocks into solutions has long been attributed to recoiling alpha-emitting nuclei. Direct evidence has been obtained for two mechanisms, first, recoil ejection from grains, and now release by natural etching of alpha-recoil tracks. The observations have implications for radon emanation and for the storage of alpha-emitting radioactive waste.*

Radioactive disequilibrium is seen in nature under many conditions among the members of the uranium and thorium decay series, in each of which alpha decay plays a prominent role. Earlier experiments on a specialized material demonstrated the presence of at least two distinct mechanisms for such separations of isotopes from their parents. Both are the result of recoiling, alpha-decaying nuclei (*1*). One of these, direct ejection of the recoiling nucleus from a grain (*1*, *2*), is physical, depends largely on the stopping power of the surroundings, and hence is insensitive to the detailed geochemical environment. It was expected that the second, radiation damage followed by chemical attack, would depend on the chemistry of pore fluids. This mechanism has now been tested and observed in a series of sensitive experiments in which implanted recoil nuclei were located by the activation of fission tracks after different minerals were exposed to various chemical solutions.

Because the natural isotopic abundances of individual elements are normally constant, the striking variability that has been observed in $^{234}U/^{238}U$ ratios on earth (*3*) is of special interest. Uranium is of interest economically with respect to nuclear energy and also geochemically because its radioactivity can be used to measure geological time by a variety of techniques in which ratios such as $^{206}Pb/^{238}U$, $^{230}Th/^{238}U$, and $^{234}U/^{238}U$ are important.

Similarly, disequilibrium between chemically different nuclides in a radioactive chain is useful both in understanding the chemical or physical environment in which the decays are occurring and in learning how to locate ore deposits or even how to predict earthquakes. As an example of the possible applications to ore discovery, the sequence of escape and migration of ^{222}Rn (a gaseous member of the ^{238}U decay chain) has been suggested as a means of locating subsurface uranium deposits (*4*), and the solution and transport of ^{226}Ra have been thought to form diffuse halos around (*5*) or displaced from (*6*) uranium deposits. In the above-described cases alpha-recoiling nuclei have frequently been invoked as the cause of disequilibrium, but direct experimental evidence on the detailed mechanism or mechanisms has been largely lacking. Recoiling nuclei from alpha emission could also affect the ease of loss of radioisotopes from nuclear waste that contains transuranic nuclides, since they are commonly alpha-emitters.

When a nucleus that is within about 200 Å of a solid surface undergoes alpha decay, the residual nucleus may recoil directly from a grain. Such behavior was first shown unambiguously by Kigoshi (*2*), who dispersed $ZrSiO_4$ crystals in various solutions and observed the build-up in the liquid of the ^{234}Th which results from the decay of ^{238}U (in turn, it decays rather quickly to ^{234}U). For wet rocks or soils this mechanism would enrich the water in ^{234}U relative to its parent ^{238}U, which tends to remain in the solid. The same process of direct recoil ejection has also been observed by a process in which a detector in vacuum is used to catch ejected ^{235}U nuclei from the decay of ^{239}Pu in PuO_2 spherules. The study established that the number of such recoils is what would be expected from the number of decays that occur in the near-surface regions of the spherules (*1*).

0036-8075/80/0229-0979$00.50/0